

Journal of Korean Institute of surface Engineering  
Vol. 29, No. 6, Dec., 1996

## SIMULTANEOUS DETERMINATION OF OPTICAL CONSTANTS AND DEPTH-PROFILE OF SPUTTERED AMORPHOUS TiO<sub>2</sub> THIN FILMS

Sung-Gyu Rhee, Soon Il Lee, and Soo-Ghee Oh

*Department of Physics, Ajou University, Suwon, 442-749, KOREA*

### ABSTRACT

Amorphous TiO<sub>2</sub> thin films were deposited on silicon substrates by the RF magnetron sputtering under various conditions, and studied by the spectroscopic ellipsometry (SE). To determine the optical constants as a function of photon energy and also to depth-profile the as-deposited TiO<sub>2</sub> thin films, we analyzed the ellipsometric spectra using the effective medium approximation and the dispersion equations. Especially, we improved the modeling accuracy by selectively using either the Sellmeier or the Forouhi and Bloomer dispersion equation in different energy regions.

### INTRODUCTION

Titanium dioxide is widely used in a variety of thin film applications due to its excellent properties. Especially, its transparency in the visible and near-IR range, high refractive index, hardness, and chemically resistant nature make TiO<sub>2</sub> ideal for the optical coatings<sup>1</sup>. For the fabrication of TiO<sub>2</sub> coatings of desirable optical properties, various deposition methods, such as chemical vapor deposition<sup>2</sup>, vacuum evaporation<sup>3, 4</sup>, ion-assisted deposition<sup>5</sup>, sol-gel processes<sup>6</sup>, and sputtering<sup>7</sup>, have been adopted. Considering the fact that the most of the widely used as-deposited TiO<sub>2</sub> thin films are amorphous regardless of their deposition methods, it is quite surprising that unlike the optical constants of the crystalline TiO<sub>2</sub> phases, those of the amorphous TiO<sub>2</sub> thin films are not very well known. The scarcity of the optical constants is particularly emi-

nent in the energy range where the extinction coefficient is not negligible.

Typically, the optical constants of the dielectric films are determined from the transmission and/or the reflectance measurements, where usually the film are assumed to be homogeneous except few cases<sup>8</sup>). Hence, in many cases the determined optical constants are not the intrinsic properties of the film, rather it includes other effects such as void fraction and surface roughness. However, spectroscopic ellipsometry has been successfully applied to the depth profiling of the dielectric films. Especially, Vedam and coworkers<sup>9</sup> were able to determine both the structure and the optical constants of the dielectric films by applying effective medium approximation while describing the refractive indices by the Sellmeier dispersion equation. Even though Vedam group's approach produced many interesting results, still there

success was somewhat limited due to the adoption of the Sellmeier dispersion equation, which intrinsically limited them to the region where the extinction coefficient is negligible.

In this paper we tried to extend Vedam group's approach to the energy region where the extinction coefficients are not negligible by employing two different dispersion equations. Particularly, we applied our analysis method to the sputtered TiO<sub>2</sub> films and investigated simultaneously the depth profile and the optical constants of the as-deposited amorphous TiO<sub>2</sub> films.

## EXPERIMENTAL

TiO<sub>2</sub> thin films were deposited at the substrate temperature of 150 °C by the RF magnetron sputtering with the sputtering power of 150 or 200 W on two different kinds of silicon substrates; the silicon substrates were either thermally oxidized or HF-etched. The thermally grown oxide layer thickness was determined as a part of the SE analysis, and listed in Table 1. Sputtering chamber has the base pressure of  $2.0 \times 10^{-6}$  torr and the working pressure was maintained at  $5 \times 10^{-3}$  torr.

Raman spectroscopy, X-ray diffraction, and spectroscopic ellipsometry (SE) were used for the structural and optical characterization of the as-deposited TiO<sub>2</sub> films. Raman spectroscopy was performed using an 5145 Å laser line up to an effective frequency shift of 1000 cm<sup>-1</sup>, X-ray diffraction was performed using a Cu target with 0.02° resolution, and photon-energy-dependent ellipsometric constant  $\Psi$ - and  $\Delta$ -spectra were measured by a Jobin-Yvon model UVISSEL spectroscopic phase modulated ellipsometer in 0.01

eV increments from 1.5 to 5.0 eV. The result of Raman scattering and X-ray Diffraction showed that the as-deposited films were all amorphous regardless of the deposition conditions. The measured  $\Psi$ - and  $\Delta$ -spectra were analyzed by a multilayer modeling to determine the optical constants and the depth-profile of the as-deposited amorphous TiO<sub>2</sub> films.

## RESULT AND DISCUSSION

The measured SE spectra are shown together with the best fit curves obtained from the multilayer modeling in Figs. 1 and 2. In multilayer modeling, the films were considered to be composed of multilayers with different thickness and void fraction, and the effective optical constants of each layer were calculated using the Bruggeman effective medium theory<sup>10</sup>. In the application of the multilayer modeling, the intrinsic optical constants of the film material are usually known, and only the multilayer structural parameters, such as thicknesses and void fractions, are determined. But as Vedam and coworkers<sup>9</sup> have shown, it is possible to include the optical constants as part of the unknown parameters and determine both the multilayer structure and the optical constants of the film from the nonlinear regression analysis (NLR). To adopt this approach, it is essential to express the intrinsic optical properties of the film material by a dispersion equation, which is required to make sure that the number of unknown parameters are smaller than the number of data in NLR. The usefulness of the Sellmeier dispersion equation in representing the refractive index  $n$  in the transparent region has been demonstrated by Vedam and coworkers,

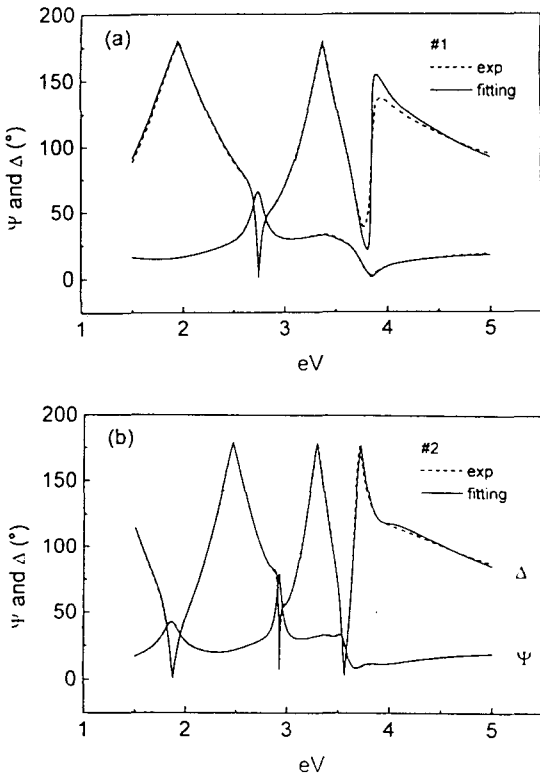


Fig. 1 The measured and the best fit SE spectra of the as-deposited amorphous  $\text{TiO}_2$  films. These films were deposited on the thermally oxidized silicon substrates at  $150^\circ\text{C}$  with the RF power of 150 W (#1) and 200 W (#2), respectively; (a) 150 W, (b) 200 W.

but it has to be emphasized that the Sellmeier dispersion equation is not applicable to the region where the extinction coefficient  $k$  is appreciable. On the other hand, the Forouhi and Bloomer dispersion equation<sup>11)</sup> which were originally developed to describe the spectral dependence of the optical constants of amorphous semiconductors and amorphous dielectrics is known appropriate to represent the optical constants in the energy region of appreciable  $k$ . However, the Forouhi and Bloomer dispersion equation has a tendency to over-

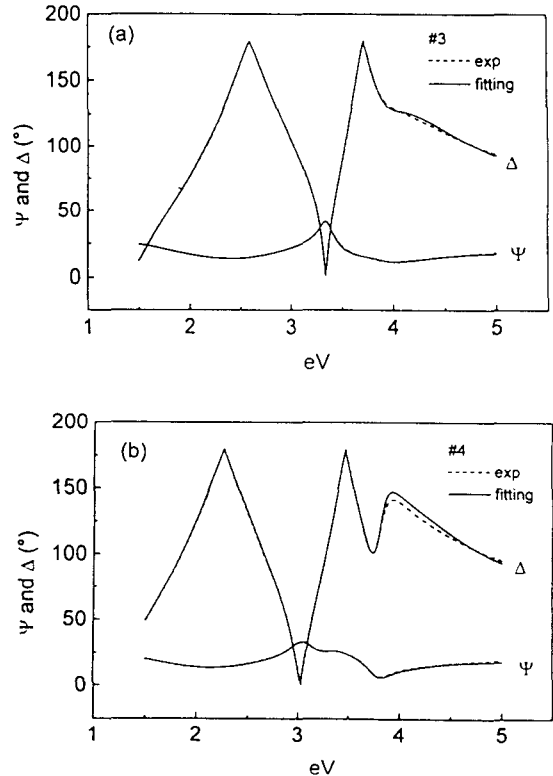


Fig. 2 The measured and the best fit SE spectra of the as-deposited amorphous  $\text{TiO}_2$  films. These films were deposited on the HF-etched silicon substrates at  $150^\circ\text{C}$  with the RF power of 150 W (#3) and 200 W (#4), respectively; (a) 150 W, (b) 200 W.

estimate  $k$  in the region far below the optical band gap. Hence, in this study we adopted the following strategy. First, we introduced the threshold energy as one of the fitting parameters. Then, we set  $k$  at zero and use the Sellmeier dispersion equation to express  $n$  below the threshold energy. Above the threshold energy, we employed the Forouhi and Bloomer dispersion equation to represent  $n$  and  $k$ . The thickness and void fraction of each layer and the optical constants of the amorphous  $\text{TiO}_2$  were determined by NLR analysis

in which Levenberg–Marquardt algorithm<sup>12)</sup> was used to minimize a value of  $\chi^2$ , the unbiased estimator of the goodness of fit<sup>10)</sup>. Since the measured spectra can not be fitted with the single layer structure, we introduced the two- or the three-layer structure which produced very good fits for all the films. The summary of the SE spectra analysis results are presented in Table 1.

Interestingly, films deposited on the different substrates exhibit different multilayer structures; ones (#1, #2) deposited on the thermally oxidized silicon substrates were fitted with a two-layer model, but the others (#3, #4) deposited on the HF-etched silicon substrates were fitted with a three-layer model. For the films #1 and #2, the fitting results show that the two films have the similar layer-structure in spite of the difference in the sputtering power, and also that the films are homogeneous except the surface roughness. For the films #3 and #4, we find that there are some differences in the layer-structure. The film #3 has the interface layer which is less dense than the bulk-like layer just above it and also the roughness layer at the surface. However, the film #4 exhibit the decrease of the void fraction from

the interface layer with large void fraction to the void-free surface layer. We attribute the observed big difference in the interfaces layer void fraction between films #1, #2 and #3, #4 to the different surface state of the substrate. We propose that the thermal oxidation has produced smooth and homogeneous surfaces suitable for the uniform nucleation, but HF-etching produced uneven surfaces which result in the growth of the porous layer.

In Fig. 3, we present the optical constants of the films #1-#4 which were determined from the SE spectra analysis discussed above. In this figure, we also show the optical constants of the rutile and the anatase which are the crystalline phase of the TiO<sub>2</sub> for comparison. From this figure, it can be seen that not only the refractive indices but also the extinction coefficient were successfully determined. The validity of the determined optical constants can be appreciated from the good fitting results shown in Figs. 1 and 2, even in the energy range where the extinction coefficients are not negligible. The most surprising feature in Fig. 3 is the close resemblance between the optical constants of film #1 and those of film #2, and also between the optical constants of film #3 and those of film #

Table 1. Summary of the SE analysis of the sputtered amorphous TiO<sub>2</sub> films.

Sample ID	Substrate	Power (W)	$\sigma$	d1 (Å)	f1 (%)	d2 (Å)	f2 (%)	d3 (Å)	f3 (%)
#1	SiO <sub>2</sub> (429 Å)/c-Si	150	0.024	77	10.01	992	0.00	–	–
#2	SiO <sub>2</sub> (470 Å)/c-Si	200	0.026	64	32.81	1284	0.00	–	–
#3	HF-etched c-Si	150	0.010	34	18.16	890	0.05	104	21.09
#4	HF-etched c-Si	200	0.014	306	0.00	776	3.32	127	39.46

where d1, d2, d3 and f1, f2, f3 represent the thicknesses and the void volume fractions of the each layer, respectively. N.B. The structure used in the modeling is the 5 phase system of air/first layer (d1, f1)/second layer(d2, f2)/third layer(d3, f3) (or oxide layer)/c-Si substrate.

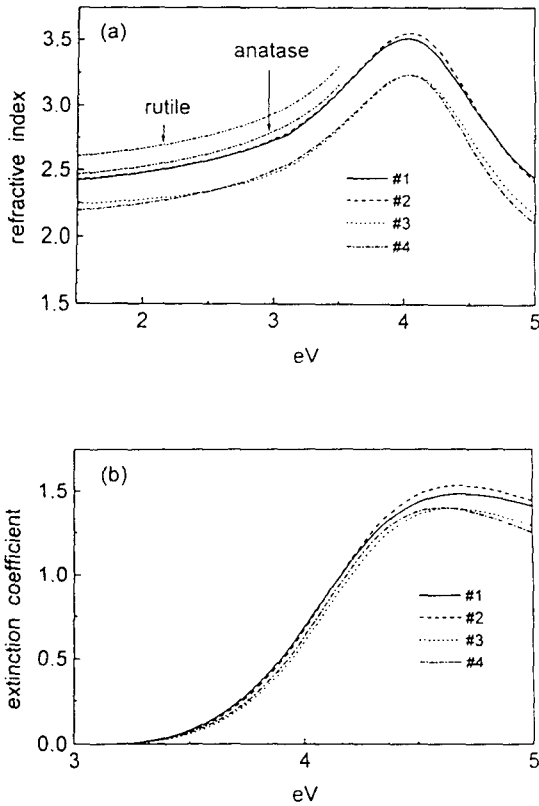


Fig. 3 The optical constants of the as-deposited amorphous  $\text{TiO}_2$  films; (a) Refractive indices, (b) Extinction coefficients. For the comparison, the refractive indices of the rutile and anatase phase of  $\text{TiO}_2$  are also shown.

4. This observation strongly suggest that the films grown on the similar substrates have the similar characteristics. But the comparison between the different films are not very straightforward, since we also treat the optical constants as fitting parameters. For example, the comparison of the void fraction between the each layer of the same film is very obvious. But it is not very clear whether the surface layer of film #4 is really denser than the surface layer of film #1. Rather the uniform downshift of the refractive indices

for all energies imply that films #3 and #4 are not as dense as films #1 and #2. We also find that all the as-deposited amorphous  $\text{TiO}_2$  films exhibit the refractive indices that lie below those of the crystalline phases. Hence in many cases, the optical data of the amorphous  $\text{TiO}_2$  films can be approximated by the mixture of void and crystalline  $\text{TiO}_2$  in the transparent region. But in the higher energy region, the analysis method like ours are essential for the accurate understanding of the measurement results. One way to characterize the amorphous phase and compare it with the crystalline phase is to determine the magnitude of the optical band gap, which can be easily done from the Tauc's plot;  $(\alpha E)^{1/2} = B(E - E_g)$ , where  $\alpha$  is the absorption coefficient. The optical band gap  $E_g$  can be deduced from the intercept of the extrapolated straight lines with the  $E$  axis as shown in Fig. 4. In this figure we find that regardless of the substrate state, the optical band gap is larger than 3.35 eV.

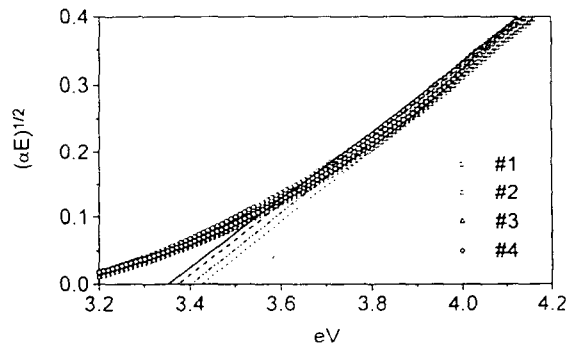


Fig. 4 Tauc's plot for the as-deposited amorphous  $\text{TiO}_2$  films.

## CONCLUSIONS

By employing multilayer modeling, we were able to determine the optical constants and the depth-profile of the sputtered amorphous TiO<sub>2</sub> films, simultaneously. The major difference between our approach and the previous approaches lies in the way we represent the optical constants of amorphous TiO<sub>2</sub>; we selectively used either the Sellmeier or the Forouhi and Bloomer dispersion equation in the energy regions where the respective dispersion equation is more appropriate.

The refractive indices of amorphous TiO<sub>2</sub> are found to have smaller values than those of the crystalline TiO<sub>2</sub>, but to have similar dispersion with those of the crystalline TiO<sub>2</sub>. Also, we find that the optical band gap of amorphous TiO<sub>2</sub> is larger than 3.35 eV from the Tauc's plot.

## ACKNOWLEDGMENTS

This paper was supported by '95 SPECIAL FUND for UNIVERSITY RESEARCH INSTITUTE, Korea Research Foundation. We also acknowledge Ajou University Basic Science Research Support Program.

## REFERENCES

1. H. K. Pulker, *Appl. Opt.* 18, (1979) 1969.
2. E. T. Fitzgibbons, K. J. Sladek, and W. H. Hartwig, *J. Electrochem. Soc.* 119, (1972) 735.
3. K. N. Rao, M. A. Murthy, and S. Mohan, *Thin Solid Films* 176, (1989) 181.
4. K. N. Rao and S. Mohan, *J. Vac. Sci. Technol. A* 8, (1990) 3260.
5. S. Miyake, T. Kobayashi, M. Satou and F. Fujimoto, *J. Vac. Sci. Technol. A* 9, (1991) 3036.
6. K. A. Vorotilov, E. V. Orlova, and V. I. Petrovsky, *Thin Solid Films* 207, (1989) 180.
7. M. H. Suhail, G. M. Rao, and S. Mohan, *J. Appl. Phys.* 71, (1992) 1421.
8. J. C. Manificier, J. Gasiot, and J. P. Fillard, *J. Phys. E: Sci. Instrum.* 9, (1976) 1002.
9. P. Chindaudom and K. Vedam, *Appl. Opt.* 33, (1994) 2664.
10. D. E. Aspnes, *SPIE* 276, (1981) 188.
11. A. R. Forouhi and I. Bloomer, *Phys. Rev. B* 34, (1986) 7018.
12. W. H. Press, B. P. Flannery, S. A. Teukolsky, and W. T. Vetterling, *Numerical Recipes* (Cambridge University Press, New York, 1986) 1st. ed, Chap. 14.